(27) A. Abragam and B. Bleaney, "Electron Paramagnetic Resonance of Transition Ions", Clarendon Press, Oxford, 1970.
(28) R. L. Carlin, C. J. O'Connor, and S. N. Bathia, *J. Am. Chem. Soc.*, **98**, 685 (1976).
(29) R. J. Kurland and B. R. McGarvey, *J. Magn. Reson.*, **2**, 286 (1970).
(30) W. D. W. Horrocks, Jr., *Inorg. Chem.*, **9**, 690 (1970).
(31) B. J. Hathaway and D. E. Billing, *Coord. Chem. Rev.*, **5**, 143 (1970).
(32) W. B. Lewis and L. O. Morgan, *Transition Met. Chem.*, **4**, 33 (1968).

Contribution from the Department of Chemistry,
Columbia University, New York, New York 10027

^{17}O Nuclear Magnetic Resonance Spectroscopy of Polyoxometalates. 1. Sensitivity and Resolution

M. FILOWITZ, R. K. C. HO, W. G. KLEMPERER,*[1] and W. SHUM

Received August 23, 1978

Over 100 ^{17}O NMR chemical shifts are reported for 27 diamagnetic polyoxoanions of the early transition metals. Efficient procedures for obtaining ^{17}O-enriched compounds are described, and the factors which control sensitivity and spectral resolution are examined and discussed in detail. Comparisons of chemical shift values with structural data show that chemical shifts are determined largely by metal–oxygen bond strengths.

Introduction

The early transition metals vanadium, niobium, tantalum, molybdenum, and tungsten in their highest oxidation states are known to form a wide variety of polynuclear metal–oxygen complexes.[2] X-ray crystallographic studies have yielded solid-state structures for several of these species, but solution structures have in many cases remained ambiguous due to the rapid and complex structural equilibria which often prevail in solution. The ^{17}O NMR technique was first successfully applied to polyoxoanion chemistry in 1965 by two groups in independent investigations of the aqueous $Cr_2O_7^{2-}$ anion.[3] Due to sensitivity problems, however, little progress was possible until the advent of Fourier transform NMR (FT NMR) spectroscopy. Since 1975, this technique has enabled ^{17}O NMR spectra of polyvanadates, -niobates, -tantalates, -molybdates, and -tungstates to be obtained.[4–16]

In this paper, we attempt to delineate the scope and limitations of the ^{17}O NMR technique as a structural and dynamic probe in polyoxoanion chemistry. First, the factors which influence spectral resolution and sensitivity are discussed, and experimental procedures for optimizing spectral quality are outlined. Next, the 13.5-MHz ^{17}O NMR spectra of a variety of diamagnetic polyoxometalates measured in solution under various conditions are presented and compared. Finally, these results are briefly summarized and areas for future investigation defined.

Experimental Section

A. Spectral Measurements. ^{17}O NMR spectra were recorded at 13.51 MHz using the pulse FT NMR technique on a Jeol PFT/PS-100 NMR spectrometer interfaced with a Nicolet 1080 data system. All spectra were digitized using 4096 data points such that digital spectrometer resolution varied between 3.7 and 4.9 Hz/data point, depending on the spectral bandwidth employed. The spectrometer was locked on the ^{1}H resonance of an external H_2O sample. Spectra were obtained using cylindrical 10-mm o.d. sample tubes (1.1-mL sample volume) and referenced externally to pure H_2O at 25 °C by the sample replacement method. Chemical shifts were calculated in parts per million, with positive values in the low field direction relative to H_2O. The error associated with chemical shift values is ±3 ppm for line widths <200 Hz, ±5 ppm for line widths >200 Hz and <400 Hz, and ±7 ppm for line widths >400 Hz. All line widths reported below in hertz have been corrected for exponential line broadening. The error associated with line-width values is ±20 Hz for line widths <100 Hz, ±40 Hz for line widths >100 Hz and <400 Hz, and ±60 Hz for line widths >400 Hz. Unless otherwise indicated, samples were neither rotated nor degassed since such precautions were found to have no measurable effect on line widths.

B. Spectral Parameters. In this section, spectra are numbered as indicated in column one of Tables II and III. The following abbreviations are used: cpd for compound, sol for solvent, |X| for molar concentration of X, *T* for temperature in °C, enr for ^{17}O content in atom percent ^{17}O, np for number of pulses, pr for pulse repetition frequency in hertz, bdw for spectral bandwidth in hertz, and exp for exponential line broadening in hertz. All pH measurements were made at 25 °C.

1: cpd = $[(n\text{-}C_4H_9)_4N]_2Mo_6O_{19}$, sol = $(CH_3)_2NCHO$, |Mo| = 1.4, *T* = 25, enr = 0.9, np = 5729, pr = 2.4, bdw = 15152, exp = 9.

2: cpd = $[(n\text{-}C_4H_9)_4N]_2Mo_6O_{19}$, sol = CH_3CN, |Mo| = 0.1, *T* = 80, enr = 20, np = 4096, pr = 7.1, bdw = 15152, exp = 2.

3: cpd = $[(n\text{-}C_4H_9)_4N]_2W_6O_{19}$, sol = $(CH_3)_2NCHO$, |W| = 0.52, *T* = 25, enr = 2, np = 9926, pr = 1.5, bdw = 15152, exp = 24.

4: cpd = $K_7HNb_6O_{19}\cdot 13H_2O$, sol = H_2O (pH 14), |Nb| = 5, *T* = 100, enr = 3, np = 1046, pr = 5.0, bdw = 15152, exp = 24.

5: cpd = $K_8Ta_6O_{19}\cdot 17H_2O$, sol = H_2O (pH 14), |Ta| = 1.2, *T* = 25, enr = 3, np = 7000, pr = 2.2, bdw = 15152, exp = 24.

6: cpd = $[(n\text{-}C_4H_9)_4N]_3VMo_5O_{19}$, sol = CH_3CN, |Mo| = 0.4, *T* = 80, enr = 10, np = 16 384, pr = 6.7, bdw = 20 000, exp = 11.

7: cpd = $[(n\text{-}C_4H_9)_4N]_3VW_5O_{19}$, sol = CH_3CN, |W| = 0.3, *T* = 30, enr = 18, np = 14 926, pr = 8.3, bdw = 20 000, exp = 8.

8: cpd = $\alpha\text{-}[(n\text{-}C_4H_9)_4N]_4SiMo_{12}O_{40}$, sol = CH_3CN, |Mo| = 0.4, *T* = 85, enr = 9, np = 32 768, pr = 8.3, bdw = 20 000, exp = 31.

9: cpd = $\alpha\text{-}[(n\text{-}C_4H_9)_4N]_4SiW_{12}O_{40}$, sol = CH_3CN, |W| = 0.4, *T* = 90, enr = 10, np = 18 204, pr = 6.7, bdw = 20 000, exp = 31.

10: cpd = $\alpha\text{-}[(n\text{-}C_4H_9)_4N]_4SiMoW_{11}O_{40}$, sol = CH_3CN, |W| = 0.3, *T* = 90, enr = 25, np = 65 536, pr = 3.1, bdw = 20 000, exp = 31.

11: cpd = $\alpha\text{-}[(n\text{-}C_4H_9)_4N]_3PMo_{12}O_{40}$, sol = CH_3CN, |Mo| = 0.5, *T* = 80, enr = 30 (phosphate oxygens), enr = 3 (remaining oxygens), np = 184 978, pr = 3.2, bdw = 20 000, exp = 31.

12: cpd = $\alpha\text{-}[(n\text{-}C_4H_9)_4N]_3PW_{12}O_{40}$, sol = CH_3CN, |W| = 0.6, *T* = 80, enr = 2, np = 32 768, pr = 7.7, bdw = 15 152, exp = 24.

13: cpd = $\alpha\text{-}[(C_4H_9)_4N]_{11}H(P_2W_{18}O_{62})_2$, sol = CH_3CN, |W| = 0.5, *T* = 85, enr = 4, np = 131 072, pr = 7.7, bdw = 15 152, exp = 24.

14: cpd = $\beta\text{-}[(n\text{-}C_4H_9)_4N]_{11}H(P_2W_{18}O_{62})_2$, sol = CH_3CN, |W| = 0.4, *T* = 90, enr = 4, np = 262000, pr = 7.7, bdw = 15 152, exp = 24.

15: cpd = $[(n\text{-}C_4H_9)_4N]_4(C_6H_5As)_4Mo_{12}O_{46}\cdot H_2O$, sol = CH_3CN, |Mo| = 0.5, *T* = 94, enr = 25, np = 9915, pr = 3.1, bdw = 20 000, exp = 47.

16: cpd = $[(n\text{-}C_4H_9)_4N]_4H_4As_4Mo_{12}O_{50}\cdot 5H_2O$, sol = CH_3CN, |Mo| = 0.6, *T* = 80, enr = 25, np = 1119, pr = 3.1, bdw = 20 000, exp = 31.

17: cpd = $[(n\text{-}C_4H_9)_4N]_2(CH_3)_2AsMo_4O_{15}H$, sol = CH_3CN, |Mo| = 0.9, *T* = 80, enr = 25, np = 4734, pr = 3.2, bdw = 20 000, exp = 47.

18: cpd = $[(n\text{-}C_4H_9)_4N]_2(C_6H_5)_2AsMo_4O_{15}H$, sol = CH_3CN, |Mo| = 0.9, *T* = 80, enr = 25, np = 16 000, pr = 3.2, bdw = 20 000, exp = 31.

19: cpd = $[(n\text{-}C_4H_9)_4N]_4W_{10}O_{32}$, sol = CH_3CN, |W| = 2.5, *T* = 25, enr = 2, np = 16 384, pr = 2.9, bdw = 15 152, exp = 12.

20: cpd = $\beta\text{-}[(n\text{-}C_4H_9)_4N]_3KMo_8O_{26}\cdot 2H_2O$, sol = CH_3CN, |Mo| = 0.05, *T* = 25, enr = 34, np = 131 072, pr = 3.2, bdw = 20 000, exp = 23.

0020-1669/79/1318-0093$01.00/0 © 1979 American Chemical Society

21: cpd = $(NH_4)_6Mo_7O_{24}\cdot 4H_2O$, sol = H_2O (pH 5.4), |Mo| = 2.5, *T* = 25, enr = 2, np = 8192, pr = 3.0, bdw = 15 152, exp = 24.

22: cpd = $Na_6Mo_7O_{24}\cdot 4H_2O$, sol = H_2O (pH 5.5), |Mo| = 2.8, *T* = 25, enr = 3, np = 12 844, pr = 3.0, bdw = 15 152, exp = 24.

23: cpd = $H_8CeMo_{12}O_{42}\cdot 18H_2O$, sol = H_2O (pH 1), |Mo| = 3.1, *T* = 25, enr $\simeq$ 15 (see below), np = 12 288, pr = 6.7, bdw = 20 000, exp = 24.

24: cpd = α-$[(n\text{-}C_4H_9)_4N]_4Mo_8O_{26}$, sol = hydrated CH_3CN, |Mo| = 0.15, *T* = 4, enr = 25, np = 8192, pr = 3.2, bdw = 20 000, exp = 11.

25: cpd = $Na_6TeMo_6O_{24}\cdot 2H_2O$, sol = H_2O (pH 5.8), |Mo| = 8.6, *T* = 82, enr = 0.4, np = 4465, pr = 3.0, bdw = 15 152, exp = 24.

26: cpd = $Na_5IMo_6O_{24}\cdot 3H_2O$, sol = H_2O (pH 5.0), |Mo| = 2.8, *T* = 100, enr = 2, np = 1029, pr = 1.8, bdw = 15 152, exp = 8.

27: cpd = $Na_3H_6AlMo_6O_{24}\cdot 4H_2O$, sol = H_2O (pH 4.1), |Mo| = 1.0, *T* = 70, enr = 3, np = 19 707, pr = 3.1, bdw = 15 152, exp = 24.

28: cpd = $Na_3H_6CoMo_6O_{24}\cdot 5H_2O$, sol = H_2O (pH 2.6), |Mo| = 1.2, *T* = 93, enr = 3, np = 10 320, pr = 3.0, bdw = 15 152, exp = 24.

29: cpd = $[(n\text{-}C_4H_9)_4N]_2Mo_2O_7$, sol = CH_3CN, |Mo| = 0.8, *T* = 25, enr = 9, np = 9504, pr = 6.3, bdw = 15 152, exp = 24.

C. **Sample Preparations.** For spectral measurements, CH_3CN (Aldrich Gold Label) solvent was distilled from CaH_2, and $(CH_3)_2NCHO$ (Pierce silylation grade) solvent was used without further purification. ^{17}O-enriched water was purchased from Miles Laboratories and Monsanto Research Corp. Enriched water recovered from aqueous syntheses was purified by distillation and analyzed for ^{17}O content using procedures described elsewhere.[17] All preparative procedures involving ^{17}O-enriched water were carried out in closed systems in order to prevent isotopic dilution by atmospheric water. $(n\text{-}C_4H_9)_4NCl$ (Eastman Organic Chemical) was recrystallized[18] and $C_6H_5AsO_3H_2$ was filtered through activated charcoal and recrystallized from 1:1 (v/v) ethanol–water before use. Fisher certified reagent $(NH_4)_6Mo_7O_{24}\cdot 4H_2O$ was recrystallized by cooling an aqueous solution, saturated at 25 °C, to 0 °C. Anal. Calcd: N, 6.80; H, 2.61; Mo, 54.34. Found: N, 6.83; H, 2.67; Mo, 54.18. All other reagents employed were the best commercial grades available and were not purified before use. Elemental analyses were performed by Galbraith Laboratories on unenriched samples.

The literature references accompanying several of the compounds listed below refer to the original preparations upon which our preparations were based. In each case, preparative conditions were adjusted in order to achieve optimum product purity, minimum degree of product hydration, and/or maximum yield of product per quantity of ^{17}O-enriched water employed. Product identity was confirmed by comparison of IR and/or Raman spectra with literature spectra.

$[(n\text{-}C_4H_9)_4N]_2Mo_6O_{19}$. A solution of 0.40 g of α-$[(n\text{-}C_4H_9)_4N]_4Mo_8O_{26}$ and 0.4 mL of ^{17}O-enriched water in 20 mL of CH_3CN was stored for 1 h. After addition of 0.05 mL of 12 N aqueous HCl, the solution volume was reduced to ca. 8 mL. Cooling of the mixture to 0 °C yielded 0.25 g of product as yellow needles which were air-dried. Anal. Calcd: C, 28.17; H, 5.31; N, 2.05; Mo, 42.19. Found: C, 28.38; H, 5.44; N, 1.99; Mo, 40.96.

$[(n\text{-}C_4H_9)_4N]_2W_6O_{19}$. ^{17}O-enriched $[(n\text{-}C_4H_9)_4N]_4W_{10}O_{32}$ (1.5 g) was refluxed in a mixture of 8 mL of CH_3CN and 30 mL of CH_3OH for 24 h. Upon cooling of the mixture to 0 °C, a precipitate formed which was filtered and air-dried. Crystallization of this precipitate from a 60 °C, saturated acetone solution cooled to 25 °C yielded 0.21 g of product as clear and colorless, block-shaped crystals. Anal. Calcd: C, 20.31; H, 3.84; N, 1.48; W, 58.30. Found: C, 20.52; H, 3.90; N, 1.43; W, 58.21.

$K_7HNb_6O_{19}\cdot 13H_2O$.[19] Nb_2O_5 (13.3 g) was added slowly to a melt of 26 g of KOH pellets (85% KOH) in a nickel crucible. After 30 min of heating, the melt was cooled to room temperature and dissolved in 100 mL of degassed water. After filtering of the mixture, the solution volume was reduced to ca. 50 mL. Needle-shaped crystals formed after 12 h at 0 °C. These crystals were filtered off, washed with 1:1 (v/v) ethanol–water and absolute ethanol, and dried in vacuo to yield 12.4 g of product. Anal. Calcd: K, 19.97; Nb, 40.68; H_2O, 17.73. Found: K, 20.13; Nb, 40.55; H_2O, 17.60.

Enriched compound was obtained by allowing a solution in ^{17}O-enriched water to stand for 12 h at 25 °C.

$K_8Ta_6O_{19}\cdot 17H_2O$.[20] Ta_2O_5 (10 g) was added slowly to a melt of 40 g of KOH pellets (85% KOH) in a nickel crucible. After 30 min of heating, the melt was cooled to room temperature and dissolved in 100 mL of degassed water. After filtering of the mixture, the solution volume was reduced to ca. 25 mL. Crystals which formed after 12 h at 0 °C were filtered off, washed with 1:1 (v/v) ethanol–water and absolute ethanol, and dried in vacuo to yield 9.3 g of product. Anal. Calcd: K, 15.57; Ta, 54.05; H_2O, 15.39. Found: K, 15.68; Ta, 53.60; H_2O, 15.30.

Enriched compound was obtained by heating an aqueous solution in ^{17}O-enriched water to 80 °C for 12 h.

$[(n\text{-}C_4H_9)_4N]_3VMo_5O_{19}$. V_2O_5 (0.11 g) and 0.08 mL of ^{17}O-enriched water were added to 30 mL of a 0.1 M $(n\text{-}C_4H_9)_4NOH$ solution in CH_3OH. After the mixture was stirred for 24 h at 25 °C, the solution was added to a solution of 1.5 g of ^{17}O-enriched α-$[(n\text{-}C_4H_9)_4N]_4Mo_8O_{26}$ in 20 mL of CH_3CN, and the resulting solution was refluxed for 6 h. Ca. 0.5 g of crude product obtained by slow addition of ether was crystallized from a saturated, 60 °C CH_3CN solution cooled to 25 °C, yielding 0.38 g of orange crystals. Anal. Calcd: C, 36.91; H, 6.97; N, 2.69; V, 3.26; Mo, 30.71. Found: C, 37.01; H, 6.90; N, 2.80; V, 3.38; Mo, 30.92.

$[(n\text{-}C_4H_9)_4N]_3VW_5O_{19}$. V_2O_5 (0.08 g) and 0.06 mL of ^{17}O-enriched water were added to 20 mL of a 0.1 M solution of $(n\text{-}C_4H_9)_4NOH$ in CH_3OH. After stirring of the mixture for 24 h at 25 °C, the solution was added to a solution of 1.3 g of ^{17}O-enriched $[(n\text{-}C_4H_9)_4N]_4W_{10}O_{32}$ in 8 mL of CH_3CN, and the resulting solution was refluxed for 24 h. Crude product, obtained by slow addition of ether, was crystallized from a saturated, 80 °C CH_3CN solution cooled to 25 °C, yielding 0.47 g of bright lemon yellow crystals. Anal. Calcd: C, 28.80; H, 5.44; N, 2.10; V, 2.55; W, 45.93. Found: C, 28.94; H, 5.47; N, 2.17; V, 2.63; W, 45.70.

α-$[(n\text{-}C_4H_9)_4N]_4SiMo_{12}O_{40}$.[21] $Na_2SiO_3\cdot 9H_2O$ (0.04 g) and $Na_2MoO_4\cdot 2H_2O$ (0.40 g) were dissolved in 1.3 mL of ^{17}O-enriched water and stored at 25 °C for 12 h. Aqueous HCl (6 N) was then added dropwise with stirring until the solution pH was <2 and the acidified solution was heated to 80 °C for 20 min. After cooling of the solution to 25 °C, 0.19 g of $(n\text{-}C_4H_9)_4NBr$ was added and the resulting precipitate was filtered off after 15 min of stirring. The yellow precipitate was washed with water, ethanol, and ether and dried in vacuo. Crystalline product (0.20 g) was obtained by cooling an 80 °C, saturated CH_3CN solution of crude product by 25 °C. Anal. Calcd: C, 27.56; H, 5.20; H, 2.01; Si, 1.01; Mo, 41.28. Found: C, 27.39; H, 5.32; N, 2.05; Si, 0.88; Mo, 40.67.

α-$[(n\text{-}C_4H_9)_4N]_4SiW_{12}O_{40}$.[22] $Na_2SiO_3\cdot 9H_2O$ (0.06 g) and $Na_2WO_4\cdot 2H_2O$ (0.80 g) were dissolved in 1.4 mL of ^{17}O-enriched water and stored at 25 °C for 12 h. The solution was then heated to ca. 60 °C, 0.25 mL of 12 N aqueous HCl was added dropwise with stirring, the solution temperature was raised to 80 °C for 30 min, and 12 N HCl was added until the solution pH was <1. After the reaction solution was refluxed for 4 h, the solution was cooled to 25 °C and 0.33 g of $(n\text{-}C_4H_9)_4NBr$ was added. The resulting precipitate was filtered after 15 min of stirring, washed with water, ethanol, and ether, and dried in vacuo. Crystalline product (0.25 g) was obtained by cooling an 80 °C, saturated CH_3CN solution of crude product to 25 °C. Anal. Calcd: C, 20.00; H, 3.78; N, 1.46; Si, 0.73; W, 57.39. Found: C, 20.21; H, 3.88; N, 1.54; S, 0.74, W, 57.35.

α-$[(C_4H_9)_4N]_4SiMoW_{11}O_{40}$.[23] $Na_2SiO_3\cdot 9H_2O$ (0.08 g) and $Na_2WO_4\cdot 2H_2O$ (1.0 g) were dissolved in 1.5 mL of ^{17}O-enriched water and stored at 25 °C for 12 h. Aqueous 12 N HCl (0.37 mL) was then added dropwise with vigorous stirring, and the resulting clear solution was refluxed for 4 h. This solution was then cooled to 25 °C (pH 6) and added to a solution of 0.067 g of $Na_2MoO_4\cdot 2H_2O$ in 0.3 mL of ^{17}O-enriched water which had been stored for 4 h. The combined reaction solution was then acidified with 6 N aqueous HCl dropwise until the solution pH was <2, $(n\text{-}C_4H_9)_4NBr$ (0.38 g) was added, and after 15 min of stirring the resulting precipitate was filtered off, washed with water and ether, and dried in vacuo. Crystalline product (0.35 g) was obtained by cooling an 80 °C, saturated CH_3CN solution of crude product to 25 °C. Anal. Calcd: Mo, 2.55; W, 53.84. Found: Mo, 2.57; W, 53.54.

α-$[(n\text{-}C_4H_9)_4N]_3PMo_{12}O_{40}$.[24] A phosphate solution was prepared by adding ca. 0.1 mL of ^{17}O-enriched water to 0.07 g of PCl_5, and a molybdate solution was prepared by dissolving 0.5 g of $Na_2MoO_4\cdot 2H_2O$ into 1.5 mL of ^{17}O-enriched water. After the molybdate solution was stored for 4 h, the two solutions were combined and acidified with 0.25 mL of 12 N aqueous HCl. $(n\text{-}C_4H_9)_4NBr$ (0.3 g) was then added, and after the mixture was stirred 15 min, the resulting precipitate was filtered off, washed with water and ether, and dried in vacuo. Crystalline product (0.22 g) was obtained by cooling an 80 °C, saturated CH_3CN solution of crude product to 25 °C. Anal. Calcd: H, 4.27; N, 1.65; P, 1.22; Mo, 45.16. Found: H, 4.33; N, 1.77; P, 1.22; Mo, 45.09.

α-[(n-C_4H_9)$_4$N]$_3$PW$_{12}$O$_{40}$.[24] A solution of 0.5 g of $Na_2WO_4\cdot 2H_2O$ in 1.0 mL of ^{17}O-enriched water was stored for 12 h at 25 °C; 0.2 mL of 85% aqueous H_3PO_4 and 0.5 mL of 12 N aqueous HCl were then added, and the resulting suspension was stirred at 25 °C for 12 h. Addition of 3 mL of water yielded a clear solution to which 0.14 g of (n-C_4H_9)$_4$NBr was added immediately. After 15 min of stirring, the resulting precipitate was filtered off, washed with water, ethanol, and ether, and dried in vacuo. Crystalline product (0.24 g) was obtained by cooling an 80 °C, saturated CH_3CN solution of crude product to 25 °C. Anal. Calcd: C, 16.00; H, 3.02; N, 1.17; P. 0.86; W, 61.21. Found: C, 16.18; H, 3.05; N, 1.20; P, 0.90; W, 61.06.

α- and β-[(n-C_4H_9)$_4$N]$_{11}$H(P$_2$W$_{18}$O$_{62}$)$_2$.[24,25] $Na_2WO_4\cdot 2H_2O$ (2.0 g) was dissolved into 4 mL of ^{17}O-enriched water and stored for 12 h at 25 °C. This solution was then heated to boiling and 2 mL of 85% aqueous H_3PO_4 was added dropwise. After refluxing of the reaction solution for 20 h, 2 drops of bromine water were added, and the solution was cooled to 25 °C. NH_4Cl (2.0 g) was then added, and the resulting precipitate was filtered and dried in vacuo. This precipitate was redissolved into 7 mL of water at ca. 50 °C and immediately reprecipitated with 2.0 g of NH_4Cl. After filtering off and drying of the precipitate, 1.44 g of crude product was obtained. This crude product is a mixture of α-$(NH_4)_6P_2W_{18}O_{62}\cdot nH_2O$ (a) and β-$(NH_4)_6P_2W_{18}O_{62}\cdot nH_2O$ (b). Pure a and b were obtained by fractional crystallization as follows. The crude product was dissolved into 3.0 mL of ^{17}O-enriched water and placed in a desiccator over concentrated H_2SO_4. Four crops of crystals were collected at intervals of about 20 h. The first crop contained 0.27 g of pure b which turned blue-green upon drying. The second crop, containing a and b, was discarded. The third and fourth crops contained 0.29 and 0.48 g of pure a, respectively. A total of 0.27 g of b was dissolved into 3 mL of water containing 1 drop of bromine water, and 0.12 g of (n-C_4H_9)$_4$NBr was added immediately. The resulting precipitate was filtered off, washed with water and ether, and dried in vacuo. This crude product was crystallized from acetone/CCl_4 by slow evaporation at 25 °C to yield 0.21 g of a yellow, crystalline β-[(n-C_4H_9)$_4$N]$_{11}$H(P$_2$W$_{18}$O$_{62}$)$_2$ after about 24 h. Anal. Calcd: C, 18.55; H, 3.51; N, 1.35; P, 1.09; W, 58.09. Found: C, 18.33; H, 3.56; N, 1.39; P, 1.05; W, 58.59.

α-[(n-C_4H_9)$_4$N]$_{11}$H(P$_2$W$_{18}$O$_{62}$)$_2$ (0.33 g) was obtained from 0.40 g of a and 0.18 g of (n-C_4H_9)$_4$NBr employing the same procedure, except that bromine water was not used. Anal. Calcd: C, 18.55; H, 3.51; N, 1.35; P. 1.09; W, 58.09. Found: C, 18.79; H, 3.54; N, 1.40; P, 1.01; W, 58.77.

[(n-C_4H_9)$_4$N]$_4$(C_6H_5As)$_4$Mo$_{12}$O$_{46}\cdot$H$_2$O. To a solution of $C_6H_5AsO_3H_2$ (0.09 g) and $Na_2MoO_4\cdot 2H_2O$ (0.34 g) in 2.5 mL of ^{17}O-enriched water was added dropwise 0.19 mL of 12 N aqueous HCl with stirring at a rate of 2 drops/min. After heating of the pH 1 reaction solution at 95 °C for 1 h in a closed system, 0.30 g of (n-C_4H_9)$_4$NBr in 0.5 mL of ^{17}O-enriched water was added. The resulting white precipitate was filtered off, air-dried for 1 h, and dried over P_2O_5 in a vacuum desiccator for 1 day. This crude product was crystallized by dissolving it into $(CH_3)_2HCHO$, adding water dropwise until faint turbidity, and then adding CH_3CN until a clear, colorless solution was obtained. After 3 days of slow evaporation at 25 °C, small crystals which had formed were filtered off and dried as just described for the crude product to yield 0.27 g of product. Anal. Calcd: C, 30.34; H, 4.80; N, 1.61; As, 8.60; Mo, 33.05. Found: C, 30.31; H, 4.85; N, 1.58; As, 8.57; Mo, 33.05.

[(n-C_4H_9)$_4$N]$_4$H$_4$As$_4$Mo$_{12}$O$_{50}\cdot$5H$_2$O.[26] H_3AsO_4 (0.16 g) was dissolved into 1.0 mL of ^{17}O-enriched water and centrifuged to remove insoluble impurities. MoO_3 (0.46 g) was added to this solution, and the suspension was heated to 100 °C for 2 h. Two drops of 3% aqueous H_2O_2 were then added to yield a yellow supernatant solution, and the entire reaction mixture was cooled to 0 °C and filtered. To the 0 °C, clear, yellow filtrate (pH 0.2), 0.35 g of (n-C_4H_9)$_4$NBr was added. The resulting pale yellow precipitate was filtered off and washed sucessively with 20 mL of 0 °C water and anhydrous ether. The product was finally air-dried for 6 days, at which time it had reached a constant weight of 0.31 g. Anal. Calcd: C, 23.19; H, 4.80; N, 1.69; As, 9.04; Mo, 34.73. Found: C, 23.35; H, 4.80; N, 1.64; As, 8.92; Mo, 34.94.

[(n-C_4H_9)$_4$N]$_2$(CH$_3$)$_2$AsMo$_4$O$_{15}$H.[27] $(CH_3)_2AsO_2H$ (1.0 g) and $Na_2MoO_4\cdot 2H_2O$ (7.0 g) were dissolved in 20 mL of water; 3.6 mL of 12 N aqueous HCl was then added to this solution at a rate of 2 drops/min with vigorous stirring. After stirring of the mixture for 1 additional hour at 25 °C a solution of (n-C_4H_9)$_4$NBr (4.0 g) in 10 mL of water was added to the pH 4 reaction solution. The resulting white precipitate was filtered off, washed successively with 50 mL of water and 50 mL of anhydrous ether, and dried in vacuo, yielding 7.6 g of crude product. Crystals were obtained by cooling an 80 °C, saturated CH_3CN solution of crude product to 25 °C. The clear, colorless crystals became opaque upon drying. Anal. Calcd: C, 33.60; H, 6.56; N, 2.31; As, 6.17; Mo, 31.60. Found: C, 33.90; H, 6.71; N, 2.32; As, 6.09; Mo, 31.49.

Enriched compound was obtained by maintaining a solution of 0.4 g of compound and 0.05 mL of ^{17}O-enriched water in 2 mL of CH_3CN at 75 °C for 70 h and then evaporating the solution to dryness. This product was then crystallized and dried as described above for the unenriched compound.

[(n-C_4H_9)$_4$N]$_2$(C$_6$H$_5$)$_2$AsMo$_4$O$_{15}$H.[27] $(C_6H_5)_2AsO_2H$ (0.73 g) and $Na_2MoO_4\cdot 2H_2O$ (2.70 g) were dissolved in 30 mL of water; 1.35 mL of 12 N aqueous HCl was then added to this solution at a rate of 2 drops/min with vigorous stirring. After stirring of the mixture for 1 additional h at 25 °C, a solution of (n-C_4H_9)$_4$NBr (1.8 g) in 5 mL of water was added to the reaction solution. The resulting precipitate was filtered off, washed successively with 30 mL of water and 30 mL anhydrous ether, and dried in vacuo, yielding 3.48 g of crude product. This crude product was recrystallized twice by cooling an 80 °C, saturated CH_3CN solution to 25 °C. The clear, colorless crystals became white upon drying. Anal. Calcd: C, 39.47; H, 6.25; N, 2.09; As, 5.60; Mo, 28.66. Found: C, 39.44; H, 6.20; N, 2.06; As, 5.75; Mo, 28.55.

Enriched compound was obtained by maintaining a solution of 0.60 g compound and 0.11 mL of ^{17}O-enriched water in 3 mL of CH_3CN at 85 °C for 19 h and then reducing the solution volume to 1.5 mL. The concentrated solution was then cooled to 0 °C for 24 h to yield 0.40 g of crystalline product.

[(n-C_4H_9)$_4$N]$_4$W$_{10}$O$_{32}$.[28] A solution of $Na_2WO_4\cdot 2H_2O$ (1.0 g) in 3 mL of ^{17}O-enriched water was stored for 12 h at 25 °C and then acidified slowly with 1.6 mL of 3 N aqueous HCl. Addition of 0.40 g of (n-C_4H_9)$_4$NCl yielded precipitate which was filtered off, washed successively with water, ethanol, and ether, and finally dried in vacuo over P_2O_5 for 24 h. Crystalline product (0.48 g) was obtained by cooling a 25 °C, saturated CH_3CN solution of crude product to 0 °C and slowly adding cold acetone. Anal. Calcd: C, 23.15; H, 4.37; N, 1.69; W, 55.37. Found: C, 23.26; H, 4.53; N, 1.83; W, 54.92.

β-[(n-C_4H_9)$_4$N]$_3$KMo$_8$O$_{26}\cdot$2H$_2$O. A saturated solution of 0.1 g of KBr in 0.18 mL of ^{17}O-enriched water was added to a solution of 0.38 g of ^{17}O-enriched α-[(n-C_4H_9)$_4$N]$_4$Mo$_8$O$_{26}$ in 10 mL of CH_3CN, and the resulting precipitate was immediately filtered off. The clear filtrate yielded 0.08 g of product as small, colorless needles after 24 h at 0 °C. Anal. Calcd: C, 29.03; H, 5.68; N, 2.12; K, 1.97; Mo, 38.65. Found: C, 29.42; H, 5.79; N, 2.26; K, 1.73; Mo, 39.43.

(NH$_4$)$_6$Mo$_7$O$_{24}\cdot$4H$_2$O. Enriched compound was obtained by dissolving recrystallized compound (see above) in ^{17}O-enriched water.

Na$_6$Mo$_7$O$_{24}\cdot$4H$_2$O.[29] MoO_3 (10.0 g) was added to a solution of NaOH (2.4 g) in 50 mL of water. The solution volume was reduced to ca. 10 mL at 50 °C, and crystals formed upon cooling the solution to 25 °C. The crystals were filtered off and dried in vacuo over P_2O_5 for 24 h. Anal. Calcd: Na, 10.86; Mo, 53.07; H, 0.64. Found: Na, 10.83; Mo, 53.12; H, 0.73.

Enriched compound was obtained by dissolving unenriched compound in ^{17}O-enriched water.

H$_8$CeMo$_{12}$O$_{42}\cdot$18H$_2$O.[30] The starting material for this preparation was $(NH_4)_8CeMo_{12}O_{42}\cdot 18H_2O$, prepared according to Shakhova and Gavrilova[31] and purified according to Baker et al.,[32] using 2% aqueous H_2SO_4 as solvent but omitting the final aqueous recrystallization. A suspension of purified ammonium salt (1.4 g) in 50 mL of water was passed through a column of H^+-form Amberlite IR-200 resin (Rohm and Haas Co.). The product acid was immediately precipitated out with 50 mL of 60% aqueous H_2SO_4, filtered off, washed six times with 60% aqueous HNO_3, washed six times with ether, and air-dried to yield 1.0 g of product (*caution*: the product should be free from HNO_3 before washing with ether, since ether and HNO_3 react violently). This compound cannot be dried in vacuo without sample decomposition. Anal. Calcd: H, 1.93; Ce, 6.10; Mo, 50.15. Found: H, 1.94; Ce, 6.35; Mo, 49.99.

Enriched compound was obtained by dissolving 0.86 g of unenriched compound into 0.40 mL of ^{17}O-enriched water and storing this solution for 24 h at 25 °C. The solution was then cooled to 0 °C and diluted with 12 mL of 0 °C water before adding 15 mL of 60% aqueous H_2SO_4 at 0 °C to precipitate out the product. After filtering off and washing of the enriched compound as described above for the unenriched compound, 0.75 g of product was obtained. The solution for ^{17}O NMR spectrum **23** was prepared by adding 0.62 g of 14% ^{17}O-enriched compound to 0.9 mL of unenriched water. The spectrum was measured immediately following preparation of the solution.

α-$[(n\text{-}C_4H_9)_4N]_4Mo_8O_{26}$. $Na_2MoO_4{\cdot}2H_2O$ (1.25 g) was dissolved into 3 mL of water and acidified with 1.0 mL of 6 N aqueous HCl to bring the solution to ca. pH 4.5. $(n\text{-}C_4H_9)_4NCl$ (0.80 g) was then added, and the resulting precipitate was filtered off and thoroughly washed successively with water, absolute ethanol, acetone, and ether. Crystalline product was obtained by dissolving the 1.05 g of crude product into 10 mL of CH_3CN at 25 °C and cooling the solution to 0 °C to obtain large clear, colorless, block-shaped crystals which lost their transparency upon drying in vacuo. The 0.78 g of pure product was stored in vacuo to prevent hydration. Anal. Calcd: C, 35.69; H, 6.75; N, 2.60; Mo, 35.64. Found: C, 35.49; H, 6.85; N, 2.60; Mo, 35.31.

Enriched compound was obtained by dissolving 0.50 g of unenriched compound and 0.50 mL of ^{17}O-enriched water into 15 mL of CH_3CN and stirring the solution at 25 °C for 1 h. Precipitation of crude product with ether followed by recrystallization from CH_3CN as described above yielded 0.34 g of pure, enriched compound.

$Na_6TeMo_6O_{24}{\cdot}2H_2O$.[33] MoO_3 (21.59 g) and $Te(OH)_6$ (5.74 g) were added to 150 mL of 1 N aqueous HCl solution, and the mixture was heated to 85 °C for 1 h. The volume of the resulting clear, colorless, ca. pH 5.8 solution was then reduced to ca. 75 mL by boiling off solvent. Cooling of the concentrated reaction solution to 25 °C produced clear colorless platelet crystals which were filtered off and dried in vacuo over P_2O_5 to yield 25.2 g of crude product. The crude product was recrystallized 8 times by cooling 85 °C, saturated aqueous solutions to 25 °C. The final batch of crystals was washed successively with absolute ethanol and anhydrous ether. After 1 day of air drying, the resulting white powder was crushed and dried in vacuo over P_2O_5 for 1 day. Anal. Calcd: Te, 10.12; Mo, 45.64. Found: Te, 9.96; Mo, 45.79.

Enriched compound was obtained by heating a solution of unenriched compound in ^{17}O-enriched water to 85 °C for 12 h.

$Na_5IMo_6O_{24}{\cdot}3H_2O$.[34] Solutions of $Na_2MoO_4{\cdot}2H_2O$ (1.35 g) in 1.0 mL of ^{17}O-enriched water and $NaIO_4$ (0.20 g) in 1.0 mL of ^{17}O-enriched water were heated separately at 95 °C for 1 h. Slow addition of 0.62 mL of 12 N HCl to the hot molybdate solution was followed by slow, dropwise addition of the hot periodate solution to the reaction solution. The volume of the resulting clear, colorless solution was reduced to 1.3 mL by boiling off solvent, and the solution temperature was then maintained at 85 °C for 12 h. Upon cooling of the mixture to 25 °C, platelet crystals appeared which were filtered off, washed successively with absolute ethanol and anhydrous ether, and air-dried to yield a white powder. The powder was crushed and dried in vacuo over P_2O_5 for 2 days. Anal. Calcd: I, 10.11; Mo, 45.85. Found: I, 10.07; Mo, 45.85.

$Na_3H_6AlMo_6O_{24}{\cdot}4H_2O$, $Na_3H_6CoMo_6O_{24}{\cdot}5H_2O$.[35] Tsigdinos' procedure was followed. Crystalline products were collected after 2 weeks for the aluminum species and after 1 week for the cobalt species, since longer times were found to yield impure products. For each compound, crystals were washed successively with anhydrous ether and absolute alcohol, air-dried, crushed, and dried in vacuo over P_2O_5 for 3 days. Anal. Calcd for $Na_3H_6AlMo_6O_{24}{\cdot}4H_2O$: Na, 6.08; Al, 2.40; Mo, 50.79. Found: Na, 6.09; Al, 2.38; Mo, 50.87. Anal. Calcd for $Na_3H_6CoMo_6O_{24}{\cdot}5H_2O$: Na, 5.83; Co, 4.98; Mo, 48.63. Found: Na, 5.80; Co, 4.95; Mo, 48.57.

Enriched samples were obtained by dissolving unenriched sample into ^{17}O-enriched water and storing the solutions for 15 h at 25 and 90 °C for the aluminum and cobalt species, respectively.

$[(n\text{-}C_4H_9)_4N]_2Mo_2O_7$. α-$[(n\text{-}C_4H_9)_4N]_4Mo_8O_{26}$ (5.0 g) and 9.5 mL of 1 N $(n\text{-}C_4H_9)_4NOH$ in CH_3OH were added to 30 mL of CH_3CN. The solution was filtered and allowed to evaporate down over 24 h to a viscous colorless oil at 25 °C. This oil was washed several times with anhydrous ether and then dissolved into 20 mL of anhydrous CH_3CN. Addition of anhydrous ether to the solution at 25 °C yielded an oil which rapidly became crystalline. The crystalline material was filtered off and washed with ether to yield 5.5 g of crude product. This crude product was then dissolved in 20 mL of anhydrous CH_3CN, and anhydrous ether (ca. 40 mL) was added with stirring until the solution became slightly cloudy. Upon cooling of the mixture to 0 °C for 12 h, large colorless crystals formed and were filtered off to yield 4.2 g of pure product. Anal. Calcd: C, 48.73; H, 9.20; N, 3.55; Mo, 24.32. Found: C, 48.85; H, 9.30; N, 3.49; Mo, 24.48.

Enriched compound was obtained by dissolving 0.80 g of unenriched compound and 0.06 mL of ^{17}O-enriched water into 6 mL of CH_3CN and stirring the solution for 1 h. Addition of ether produced a crude precipitate which was recrystallized once as outlined above to yield 0.58 g of enriched compound.

Background

The ^{17}O nucleus is a difficult nucleus to observe by NMR spectroscopy for two reasons. First, it is a spin $^5/_2$ nucleus with an appreciable electric quadrupole moment ($Q = -2.6 \times 10^{-26}$ cm^2)[36] which in general leads to rapid nuclear quadrupole relaxation. This rapid relaxation is advantageous in that it allows rapid RF pulsing using the FT NMR technique. At the same time, however, it leads to broad resonances and hence poor spectral resolution and poor signal to noise ratios. Furthermore, this rapid spin–spin relaxation necessitates the use of short delay times between the end of each RF pulse and the beginning of data collection, often resulting in incomplete spectrometer recovery and consequently baseline distortion in transformed spectra. ^{17}O NMR is also problematic due to the low natural abundance of ^{17}O (0.037%),[37] which usually necessitates the use of ^{17}O-enriched samples. Since ^{17}O is an expensive isotope, the ^{17}O NMR technique is often limited to the study of those compounds which may be efficiently enriched.

Quadrupole Relaxation. Under conditions of rapid, isotropic molecular tumbling in a homogeneous medium, the quadrupolar relaxation time T_1 for ^{17}O is determined by eq 1,[38]

$$\frac{1}{T_1} = \frac{1}{T_2} = \frac{3}{125}\left(1 + \frac{\mathbf{n}^2}{3}\right)\left(\frac{e^2Qq}{\hbar}\right)^2 \tau_c \qquad (1)$$

where $\mathbf{n}$ is the electric field gradient asymmetry parameter, $(e^2Qq/\hbar)$ is the quadrupole coupling constant, and τ_c is the correlation time for molecular rotation. Since the asymmetry parameter and the quadrupole coupling constant represent intramolecular interactions, T_1 may be increased for a given molecule only by lowering the value of τ_c, i.e., by effecting more rapid molecular tumbling. Qualitatively, the Stokes–Einstein–Debye equation[39] relates τ_c to temperature T, solution viscosity η, and molecular radius a.

$$\tau_c = 4\pi\eta a^3/3kT \qquad (2)$$

Low values of τ_c are obtained, therefore, by measuring samples at high temperature in solutions having low viscosity. Low solution viscosity is achieved by using low-viscosity solvents, low solute concentrations, and high solution temperatures.

The choice of solvent is of paramount importance if high-quality ^{17}O NMR spectra are to be obtained. Four factors must be taken into account when selecting a solvent. First, the solvent must not be reactive toward the compound to be studied if sample decomposition and/or rapid exchange processes are to be avoided. Second, the solvent must be quite polar since most polyoxometalates are polyelectrolytes and will otherwise be insoluble. Third, the solvent should have a high boiling point in order to allow spectra to be measured at elevated temperature. Finally, the solvent should have low viscosity in order to obtain long nuclear relaxation times. The properties of several solvents commonly employed in polyoxoanion chemistry are given in Table I. Although water is a very powerful solvent for highly charged polyoxoanions and also has a high boiling point, it is of limited utility because of its high viscosity and reactivity (see below). Furthermore, it always generates a strong solvent resonance which not only may obscure other resonances but also aggravates "pulse breakthrough" problems which result in poor spectral baselines

Table I. Solvent Properties[a]

solvent	viscosity, cP	bp, °C
H_2O	1.01[b]	100
1,2-$C_2H_4Cl_2$	0.80[b]	84
$(CH_3)_2NCHO$	0.80[c]	152
$CHCl_3$	0.54[c]	62
CH_2Cl_2	0.39[d]	40
CH_3CN	0.35[c]	82
$(CH_3)_2CO$	0.32[c]	56

[a] From A. J. Gordon and R. A. Ford, "The Chemist's Companion", Wiley, New York, N.Y., 1972, pp 2–16. [b] At 20 °C. [c] At 25 °C. [d] At 30 °C.

(see above). Of the remaining solvents listed in Table I, CH_3CN offers the best overall properties in terms of polarity, boiling point, and viscosity.

^{17}O Enrichment. Many polyoxoanions have sufficiently high solubilities in polar solvents as to allow FT NMR spectra to be obtained at natural ^{17}O abundance. Such highly concentrated solutions have very high viscosities, however, and the broad resonances observed usually prevent observation of fully resolved spectra. Thus although ^{17}O enrichment is not always a necessity, it always allows more dilute solutions to be studied and consequently allows greater spectral resolution to be obtained. Several procedures for ^{17}O enrichment will be outlined here, and their relative merits assessed. All of these procedures utilize commercially available ^{17}O-enriched water as the source of enrichment.

Many polyoxoanions undergo facile oxygen exchange with water and may be enriched by mixing unenriched compound with ^{17}O enriched water. This procedure is extremely efficient when it can be carried out in a nonaqueous solvent but less efficient when the enriched water must be used as the solvent. Caution must always be exercised, however, to ensure that oxygen exchange is not accompanied by sample decomposition. In addition, the possibility of site selective oxygen exchange must be taken into account, particularly when polyoxoanions contain subunits known to be inert toward oxygen exchange with water.

An alternative approach to enrichment is available when polyoxoanions can be interconverted in high yield. The compounds $[(n\text{-}C_4H_9)_4N]_2Mo_6O_{19}$ and β-$[(n\text{-}C_4H_9)_4N]_3KMo_8O_{26}\cdot 2H_2O$, for example, may be efficiently prepared from α-$[(n\text{-}C_4H_9)_4N]_4Mo_8O_{26}$ in CH_3CN. Since this starting material rapidly exchanges oxygen with water in CH_3CN, high enrichment may be obtained at low cost.

The majority of polyoxoanions are prepared by acidification of mononuclear oxoanions in aqueous solution. When the above-mentioned enrichment procedures are not applicable, one may usually resort to the alternative of synthesis by acidification of mononuclear oxoanions in ^{17}O-enriched aqueous solution since the VO_4^{3-}, MoO_4^{2-}, and WO_4^{2-} anions all undergo oxygen exchange with water. Although this method is generally inefficient, it may be optimized by using as concentrated solutions as possible and by recovering the enriched solvent water for future use.

Results and Discussion

^{17}O NMR spectra provide structural and dynamic information in terms of the line widths, intensities, and chemical shifts of observed resonances. Although line widths are usually determined by the rate of nuclear quadrupole relaxation (see above), further information may be obtained when spin–spin coupling and/or rapid oxygen exchange processes affect line widths (see below). The integrated intensities of ^{17}O NMR resonances in spectra reported here are only a qualitative measure of relative numbers of oxygen nuclei since relaxation rates for nonequivalent nuclei may vary, the RF pulse power decreases with increasing frequency from the carrier, and audio frequency filtering decreases signal intensity in the same fashion. As a general rule, intensity data are most reliable when resonances having similar line widths and chemical shifts are compared. Chemical shift data provide the most readily interpreted structural information. Although detailed interpretation of chemical shift data will not be attempted in this paper, attempts will be made to assign resonances for all compounds investigated. These assignments will be based on the general correlation between downfield chemical shift and oxygen π-bond order which has been established for several classes of oxo compounds.[40] While there is a priori no reason to believe that such a correlation should be generally valid for the diamagnetic polyoxoanions studied here, the self-consistency obtained supports the validity of the premise.

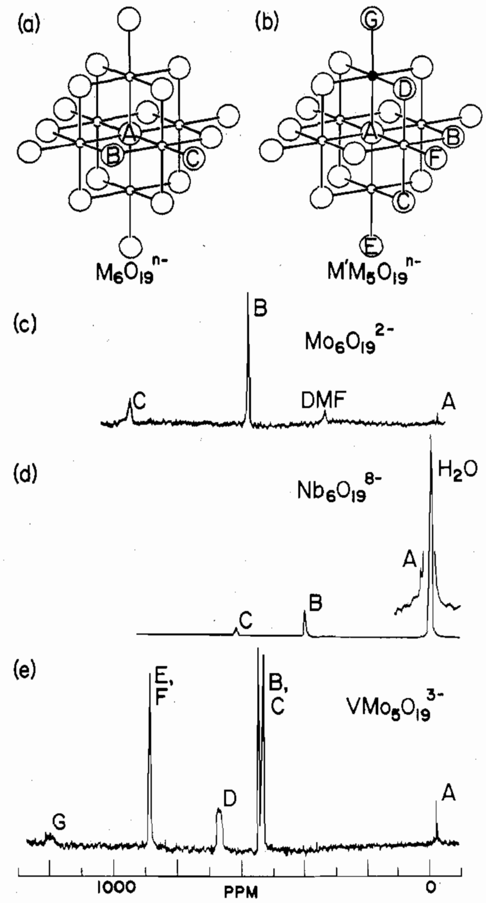

Figure 1. Idealized bond structures of (a) $M_6O_{19}^{n-}$ and (b) $M'M_5O_{19}^{n-}$ anions. Large open circles represent oxygen atoms, small open circles represent M atoms, and the small filled circle represents the M′ atom. Within each structure, one member of each symmetry-equivalent set of oxygen atoms is labeled, and this labeling scheme is used in assigning resonances in (c)–(e). The ^{17}O NMR spectra shown in (c), (d), and (e) correspond to spectra **1**, **4**, and **6**, respectively, in Table II.

Hexametalates $M_6O_{19}^{n-}$. The octahedral[41] hexametalates $M_6O_{19}^{n-}$, M = Mo^{VI}, W^{VI}, Nb^{V}, and Ta^{V}, contain only three nonequivalent types of oxygens (see Figure 1a): 6 terminal oxygens (O_C), 12 doubly bridging oxygens (O_B), and 1 sixfold bridging oxygen (O_A). ^{17}O NMR resonances (see Figure 1c,d and Table II) are assigned using the general correlation between chemical shift and π-bond order mentioned above. In the hexamolybdate ion, for example, average bond lengths[42] are 1.7, 1.9, and 2.3 Å for the O_C–Mo, O_B–Mo, and O_A–Mo bonds, respectively, and the π-bond order is assumed to increase as bond length decreases. Resonances for the other $M_6O_{19}^{n-}$ anions are assigned in an analogous fashion. Note that these assignments imply relative intensities of the three resonances which are qualitatively in agreement with the observed intensities. Furthermore, the O_A resonance is in each case assigned to the very narrow resonance in each spectrum,

Table II. 13.51-MHz ^{17}O NMR Spectral Data for Hexametalates and Keggin Anions[a]

	anion[b]	structure[c]	chemical shifts, ppm (assignments[d]) [line widths,[e] Hz]
1[b]	$Mo_6O_{10}^{2-}$ [f]	1a[42]	927 (C) [130], 559 (B) [50], −32 (A) [10]
2	$Mo_6O_{19}^{2-}$ [g]	1a[42]	933 (C) [20], 563 (B) [10]
3	$W_6O_{19}^{2-}$	1a[43]	772 (C) [100], 413 (B) [70], −81 (A) [30]
4	$Nb_6O_{19}^{8-}$	1a[44]	607 (C) [90], 392 (B) [90], 29 (A) [*h*]
5	$Ta_6O_{19}^{8-}$	1a[45]	478 (C) [140], 328 (B) [120], −39 (A) [*h*]
6	$VMo_5O_{19}^{3-}$	1b[46]	1200 (G) [390], 885 (E, F) [60], 665 (D) [250], 541, 531 (B,C) [30] [30], −22 (A) [30]
7	$VW_5O_{19}^{3-}$	1b[47]	1217 (G) [450], 731 (E, F) [120], 562 (D) [270], 395, 389 (B, C) [80],[i] −75 (A) [30]
8	α-$SiMo_{12}O_{40}^{4-}$	3a[48]	928 (D) [80], 580, 555 (B, C) [60] [130], 41 (A) [150]
9	α-$SiW_{12}O_{40}^{4-}$	3a[49]	761 (D) [130], 427, 405 (B, C) [80] [180], 27 (A) [150]
10	α-$SiMoW_{11}O_{40}^{4-}$	3a[50]	929 (D^j) [120], 762 (D^k) [130], 504, 469 ($B,^l$ C^l) [90] [130], 427, 405 ($B,^m$ C^m) [100] [200], 27 (A^n) [120]
11	α-$PMo_{12}O_{40}^{3-}$	3a[51]	936 (D) [60], 583, 550 (B, C) [90] [120], 78 (A) [490]
12	α-$PW_{12}O_{40}^{3-}$	3a[52]	769 (D) [80], 431, 405 (B, C)[o] [80] [150]

[a] See Experimental Section for spectral parameters. [b] The bold face number is used to identify each spectrum in the main text; the anion formulation given here does not take into account the degree of protonation or deprotonation which may occur in solution; see Experimental Section for solvent and counterions. [c] The first number indicates the figure in this paper which shows the anion structure; the superscript number gives the literature reference for the structure determination. [d] Parenthesized letters are assignments of the resonances using the labeling scheme given in the figure indicated in column three. [e] In brackets after assignment. [f] In *N,N*-dimethylformamide at 25 °C. [g] In acetonitrile at 80 °C. [h] Shoulder. [i] Combined line width of B and C resonances. [j] OMo. [k] OW. [l] OMoW. [m] OW_2. [n] OPW_3 and $OPMoW_2$, unresolved. [o] The O_A oxygens were not enriched in this compound and no O_A resonance was observed.

consistent with the fact that the O_A oxygen is in an octahedral environment where symmetry implies a zero electric field gradient (q in eq 1) and hence no rapid quadrupolar relaxation.

Although the $V_6O_{19}^{8-}$ ion is unknown, the mixed metal anions $VMo_5O_{19}^{3-}$ and $VW_5O_{19}^{3-}$ allow the effects of vanadium–oxygen bonding to be studied. The C_{4v} $M'M_5O_{19}^{3-}$ structure (see Figure 1b), $M' = V^V$ and $M = Mo^{VI}$ or W^{VI}, contains seven nonequivalent types of oxygens: 1 terminal OM′ oxygen (O_G), 2 types of terminal OM oxygens (O_E, O_F), 1 type of doubly bridging OM′M oxygens (O_D), 2 types of doubly bridging OM_2 oxygens (O_B, O_C), and 1 sixfold bridging $OM'M_5$ oxygen (O_A). The assignments of resonances for the $VMo_5O_{19}^{3-}$ ion given in Figure 1a and Table II are based on the following considerations. First, the very narrow −22 ppm resonance is assigned to the $OMoW_5$ oxygen by analogy with the M_6O_{19} cases discussed above. Second, the broad and flat line shapes of the 1200 and 665 ppm resonances are attributed to ^{51}V–^{17}O coupling,[53] and these resonances are assigned to the OV and OVW oxygens, respectively. Finally the resonance at 885 ppm and the pair of resonances at 541 and 531 ppm are assigned to the OMo oxygens and the two types of OMo_2 oxygens, respectively, since the chemical shift values are similar to those observed for the OMo and OMo_2 oxygens in $Mo_6O_{19}^{2-}$. Note that the resonances for the two types of OMo oxygens are not resolved and that the two resolved OMo_2 resonances cannot be unambiguously assigned due to their equal intensities. Note also that the OMo and OMo_2 resonances in $VMo_5O_{19}^{3-}$ are shifted upfield relative to the corresponding resonances in $Mo_6O_{19}^{2-}$, indicating bond weakening. This weakening of Mo–O bonds can be attributed to the larger anionic charge which is apparently delocalized over the anion to a significant extent (see below).

We have measured a series of $Mo_6O_{19}^{2-}$ spectra which show the influence of solvent, temperature, and concentration on ^{17}O NMR parameters. As might be expected for such a nonbasic[54] anion, chemical shift values undergo no significant changes when sample conditions are varied (see Table II). Line widths, however, are markedly influenced by sample conditions. The sensitivity of line width to temperature changes is illustrated by the data plotted in Figure 2. The important feature of this graph is an increase in sensitivity of line width to temperature change as the temperature is decreased. This trend is qualitatively reproduced by eq 2 and 3 which imply a direct proportionality between line width and (η/T).

The $Nb_6O_{19}^{8-}$ spectrum (see Figure 1d) exemplifies problems which may be encountered when measuring spectra from aqueous solutions. Although it would in general not be possible to observe a 29 ppm polyoxoanion resonance in aqueous solution, four mitigating conditions are present here which allow its observation. First, the $Nb_6O_{19}^{8-}$ anion has a very high solubility as a potassium salt, resulting in only a "small" water resonance which does not obscure the O_A resonance. Second, the 29 ppm resonance is unusually narrow due to the inhibition of quadrupolar relaxation at the octahedral O_A site. Third, the $Nb_6O_{19}^{8-}$ is stable in strongly basic solution, far removed from the region of neutrality where proton spin–spin coupling causes a broadening of the water resonance.[55] Finally, the $Nb_6O_{19}^{8-}$ ion is thermally stable and may be heated in order to further narrow the water resonance.

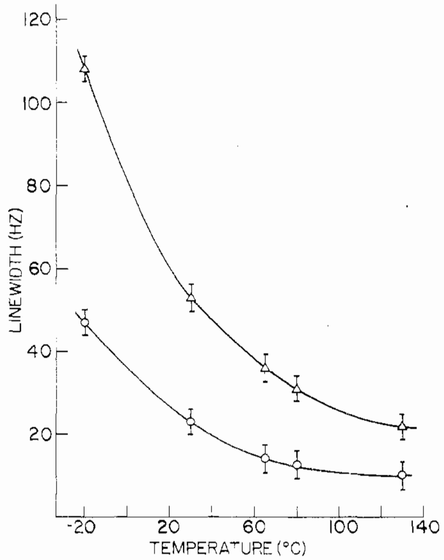

Figure 2. ^{17}O NMR line widths of the bridging oxygen resonance (○) and terminal oxygen resonance (△) from $[(n\text{-}C_4H_9)_4N]_2Mo_6O_{19}$ in $(CH_3)_2NCHO$, [Mo] = 0.09 M, as a function of temperature.

A different potential problem, site selective oxygen exchange, is encountered in the aqueous $Ta_6O_{19}^{8-}$ system. When unenriched $K_8Ta_6O_{19}\cdot 17H_2O$ is dissolved in ^{17}O-enriched water, a spectrum measured after allowing the solution to stand for 12 h at room temperature displays no O_A resonance (see Figure 1a) and an anomalous intensity ratio for the O_B and O_C resonances, i.e., an O_c resonance which is more intense than the O_B resonance. If a solution is prepared in a similar fashion but heated to 90 °C for 2 h, the O_B and O_C resonances have a normal intensity ratio corresponding to statistical oxygen

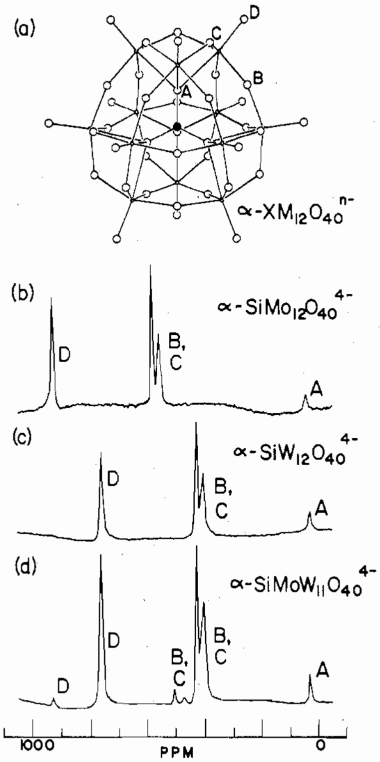

Figure 3. The α-Keggin structure[74] for anions α-$XM_{12}O_{40}$ is shown in (a), viewed approximately down a C_3 axis. Large open circles represent oxygen atoms, small open circles represent M atoms, and the large filled circle represents the X atom. One member of each symmetry-equivalent set of oxygen atoms is labeled, and this labeling scheme is used in assigning resonances in (b)–(d). The ^{17}O NMR spectra shown in (b), (c), and (d) correspond to spectra **8**, **9**, and **10** in Table II.

exchange, but the O_A resonance is still not observed. Experiments performed on the aqueous $Nb_6O_{19}^{8-}$ system, however, failed to show site selective oxygen exchange under the same experimental conditions.

Keggin Compounds α-$XM_{12}O_{40}^{n-}$. The tetrahedral Keggin anions α-$XM_{12}O_{40}^{n-}$ have the structure shown in Figure 3a. The oxygens in this structure fall into four classes of symmetry-equivalent oxygens: there are 4 OXM_3 oxygens (O_A), 12 OM_2 oxygens (O_B) each bonded to two metals whose octahedral coordination polyhedra are linked by corner sharing, 12 OM_2 oxygens (O_C) each bonded to two metals whose coordination polyhedra are linked by edge sharing, and 12 OM oxygens (O_D). The coordination geometry of the metals M in the $M_6O_{19}^{n-}$ and $XM_{12}O_{40}^{n-}$ anions is quite similar, leading to the expectation of similar chemical shift values for the two classes of compounds. In the $PW_{12}O_{40}^{3-}$ ion, for example, bond lengths are 1.704, 1.909, 1.903, and 2.435 Å for the O_D–W, O_C–W, O_B–W, and O_A–W bonds, respectively.[52] Resonances for the $SiMo_{12}O_{40}^{4-}$, $SiW_{12}O_{40}^{4-}$, $PMo_{12}O_{40}^{3-}$, and $PW_{12}O_{40}^{3-}$ anions are assigned as shown in Figure 3 and Table II assuming that oxygens with shorter bonds have greater π-bond order and hence resonances which appear further downfield. We have made no choice between the two possible assignments of the OM_2 resonances to the O_B and O_C oxygens since the M–O_B and M–O_C bond lengths are almost identical. Comparison of the chemical shift values for the OM as well as the OM_2 oxygens in the $XM_{12}O_{40}^{n-}$ anions with the chemical shift values for the corresponding types of oxygens in the $M_6O_{19}^{n-}$ anion containing the same metal shows good agreement, as expected.

When the chemical shift values for the OM as well as OM_2 resonances from $PMo_{12}O_{40}^{3-}$ and $PW_{12}O_{40}^{3-}$ are compared with the values for the corresponding resonances from $SiMo_{12}O_{40}^{4-}$ and $SiW_{12}O_{40}^{4-}$, respectively, they are observed in each case to differ by less than 10 ppm in spite of the difference in net anionic charge. This contrasts significantly with the large chemical shift differences observed when chemical shift values for the OM as well as OM_2 resonances from $Mo_6O_{19}^{2-}$ and $W_6O_{19}^{2-}$ are compared with the values for the corresponding oxygens in $VMo_5O_{19}^{3-}$ and $VM_5O_{19}^{3-}$, respectively (see above). We attribute this failure to observe large perturbations of OM and OM_2 chemical shift values when the X atom in $XM_{12}O_{40}^{n-}$ is changed from P^V to Si^{IV} to the length (>2.4 Å) and resulting weakness of the O_A–M bonds. These weak bonds apparently isolate the central XO_4^{n-} unit from the surrounding $M_{12}O_{36}$ cage to a significant extent and prevent extensive delocalization of increased negative charge to the OM and OM_2 oxygens.

We have measured the ^{17}O NMR spectrum of the α-$SiMoW_{11}O_{40}^{4-}$ anion (see Figure 3d and Table II) in order to observe the effect of metal atom substitution which does not alter net anionic charge. Although substitution of a W^{VI} by Mo^{VI} in the $SiW_{12}O_{40}^{4-}$ structure lowers the anion symmetry drastically, no measurable change in chemical shift is observed for the OW and OW_2 resonances, reflecting the localized nature of the perturbation. In addition, the OMo oxygen chemical shifts for α-$SiMoW_{11}O_{40}^{4-}$ and α-$SiMo_{12}O_{40}^{4-}$ are identical within the experimental error. Note also that each of the chemical shift values for the two OMoW resonances from α-$SiMoW_{11}O_{40}^{4-}$, 504 and 469 ppm, compares well with the average value of the corresponding OMo_2 and OW_2 chemical shift values from α-$SiMo_{12}O_{40}^{4-}$ and α-$SiW_{12}O_{40}^{4-}$, 504 and 480 ppm.

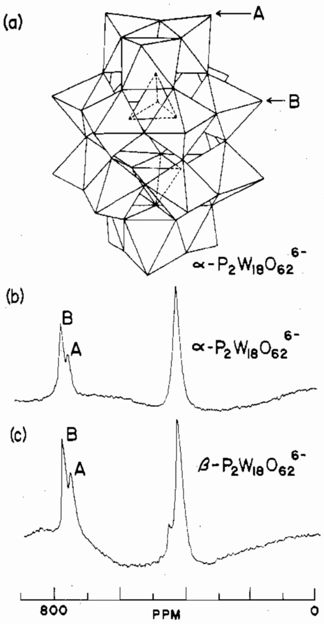

Figure 4. Polyhedral model of the α-$P_2W_{18}O_{62}^{6-}$ structure is shown in (a). Octahedra outline the octahedral tungsten coordination polyhedra; tetrahedra outline the tetrahedral phosphorus coordination polyhedra. Obscured portions of the tetrahedra are indicated by dashed lines. One member from each set of symmetry-equivalent terminal oxygen atoms is labeled, and this labeling scheme is used in (b). The ^{17}O NMR spectra shown in (b) and (c) correspond to spectra **13** and **14**, respectively, in Table III.

Other Iso- and Heteropolyanions. ^{17}O NMR spectra of other iso- and heteropolyanions are shown in Figures 4–11, and spectral data are given in Table III.

The a^3 factor in eq 2 implies that the rate of molecular tumbling decreases rapidly as the ionic radius, a, increases. The spectra of large species shown in Figure 4 display broad resonances as a result of their slow tumbling in solution.[68] In the α-$P_2W_{18}O_{62}^{6-}$ ion, only one OW_2 resonance is observed (see

Table III. 13.51-MHz ^{17}O NMR Spectral Data for Selected Iso- and Heteropolyanions[a]

	anion[b]	structure[c]	chemical shifts, ppm (assignments[d]) [line widths[e] in Hz]
13[b]	$\alpha\text{-}P_2W_{18}O_{62}^{6-}$	4a[25,56]	759 (B) [200], 738 (A) [*h*], 418 (*f*)[g] [290]
14	$\beta\text{-}P_2W_{18}O_{62}^{6-}$	- -[25,57]	757 [180], 736 [*h*], 451 [*h*], 418[g] [280]
15	$(C_6H_5As)_4Mo_{12}O_{46}^{4-}$	5a[58]	946 (E) [500], 366 (D) [390], 225 (C) [340], 103 (B) [>1000]
16	$H_4As_4Mo_{12}O_{50}^{4-}$	5a[59]	951 (E) [420], 364 (D) [560], 225 (C) [350], 90 (A, B) [>1000]
17	$(CH_3)_2AsMo_4O_{15}H^{2-}$	6a[27]	867, 855 (E, F) [230[i]], 389, 375 (C, D) [340[i]], 80 (B) [330], −15 (A) [320]
18	$(C_6H_5)_2AsMo_4O_{15}H^{2-}$	6a[27]	868, 861 (E, F) [200[i]], 390 (C, D) [180], 68 (B) [440], −10 (A) [130]
19	$W_{10}O_{32}^{4-}$	7a[60]	762 (E, F) [240], 430, 416 (B, C, D) [120] [*h*], −6 (A) [110]
20	$\beta\text{-}Mo_8O_{26}^{4-}$	8a[61]	900 (I) [*h*], 866 (E–H) [250], 743 (D) [200], 425 (C) [250], 296 (B) [200], 56 (A) [140]
21	$Mo_7O_{24}^{6-}$[j]	8b[62]	824 (F–I) [430], 759 (E) [120], 398 (C, D) [170], 340 (B) [150], 123 (A) [90]
22	$Mo_7O_{24}^{6-}$[k]	8b[62]	814 (F–I) [530], 757 (E) [150], 395 (C, D) [250], 335 (B) [230], 123 (A) [140]
23	$CeMo_{12}O_{42}^{8-}$	9a[63]	898 (C) [650], 214 (A or B) [690]
24	$\alpha\text{-}Mo_8O_{26}^{4-}$	10a[13,64]	866 (D) [350], 775 (C) [200], 495 (B) [320], 396 (A) [370]
25	$TeMo_6O_{24}^{6-}$	10b[65]	807 (C) [170], 383 (B) [170], 180 (A) [480]
26	$IMo_6O_{24}^{5-}$	10b[65]	825 (C) [50], 387 (B) [90], 255 (A) [540]
27	$H_6AlMo_6O_{24}^{3-}$	10b[66]	833 (C) [100], 378 (B)[l] [50]
28	$H_6CoMo_6O_{24}^{3-}$	10b[66]	838 (C) [60], 382 (B)[l] [90]
29	$Mo_2O_7^{2-}$	11a[15,67]	715 (B) [40], 248 (A) [200]

[a-e] See Table II, notes *a-e*. [f] Assigned to OW_2 resonances. [g] The central OPW_2 and OPW_3 oxygens were not enriched in this compound and their resonances were not observed. [h] Shoulder. [i] Combined line width of two resonances. [j] Ammonium salt. [k] Sodium salt. [l] O_A resonances not observed.

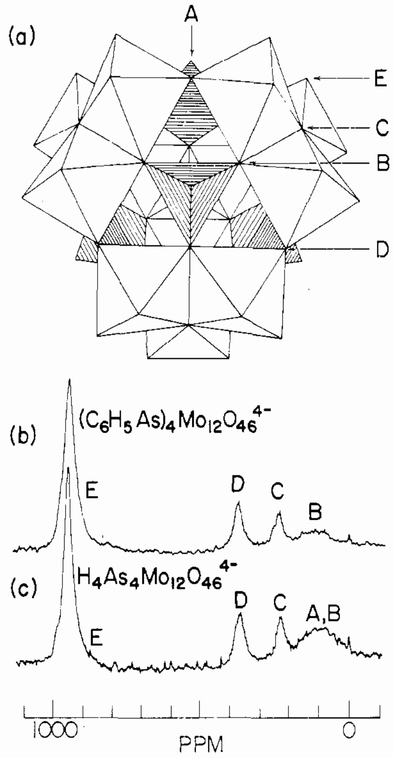

Figure 5. Polyhedral model of the tetrahedral $H_4As_4Mo_{12}O_{50}^{4-}$ structure is shown in (a). Octahedra outline the octahedral molybdenum coordination polyhedra and tetrahedra outline the tetrahedral arsenic coordination polyhedra. One member from each set of symmetry-equivalent oxygen atoms is labeled, and this labeling scheme is used in (b) and (c). In the $H_4As_4Mo_{12}O_{50}^{4-}$ structure, the O_A oxygens are protonated. In the $(C_6H_5As)_4Mo_{12}O_{46}^{4-}$ structure, the O_A sites are occupied by C_6H_5 groups. The ^{17}O NMR spectra shown in (b) and (c) correspond to spectra **15** and **16**, respectively, in Table III.

Figure 4b), even though there are five nonequivalent types of OW_2 oxygens in the structure. As a result of this low resolution, ^{17}O NMR is unable to provide any information regarding the structure of the isomeric $\beta\text{-}P_2W_{18}O_{62}^{6-}$ ion (see Figure 4c).[57] Although the $H_4As_4Mo_{12}O_{50}^{4-}$ ion shown in Figure 5a has approximately the same ionic radius as the Keggin ions (see above), it yields much broader ^{17}O resonances, presumably because its less spherically shaped surface interacts more strongly with solvent molecules, thus inhibiting molecular tumbling.[69] As expected for isostructural species having the same net charge, the $H_4As_4Mo_{12}O_{50}^{4-}$ and $(C_6H_5As)_4Mo_{12}O_{46}^{4-}$ anions exhibit chemical shift values for OMo, OMo_2, and OMo_3 oxygens which are identical within experimental error.

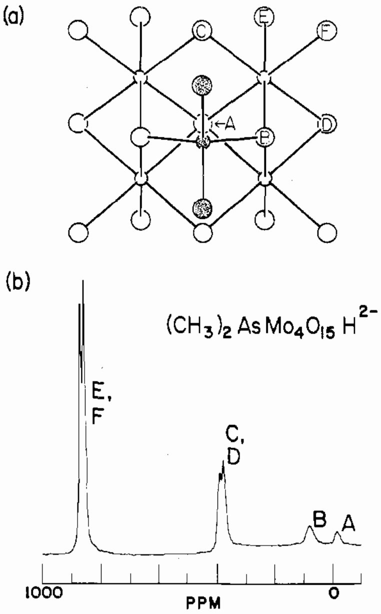

Figure 6. Idealized bond structure of $(CH_3)_2AsMo_4O_{15}H^{2-}$ is shown in (a). Large open circles represent oxygen atoms, small open circles represent molybdenum atoms, large shaded circles represent methyl groups, and the small shaded circle represents the arsenic atom. One member from each set of symmetry-equivalent oxygen atoms is labeled, and this labeling scheme is used in (b). The O_A oxygen is protonated. The ^{17}O NMR spectrum shown in (b) corresponds to spectrum **17** in Table III.

The completely resolved spectrum of $(CH_3)_2AsMo_4O_{15}H^{2-}$ (see Figure 6) demonstrates the high resolution which may be obtained from small polyoxoanions. This spectrum also illustrates the sensitivity of ^{17}O NMR chemical shifts to structural environment: the nonequivalent OMo and OMo_2 oxygen resonances are resolved even though the average Mo–O bond lengths for the nonequivalent OMo and the nonequivalent OMo_2 oxygens differ by less than 0.003 Å and 0.001 Å, respectively.[27,70] Clearly, other factors besides bond lengths must

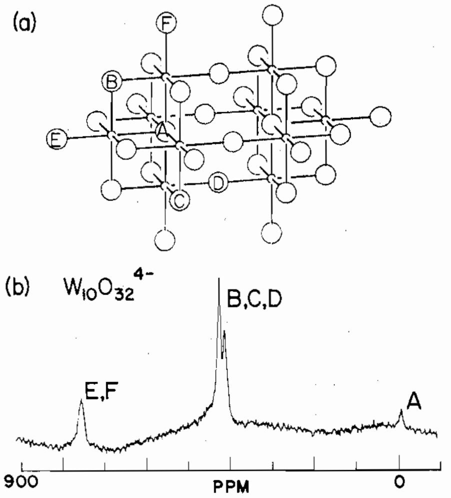

Figure 7. Idealized bond structure of $W_{10}O_{32}^{4-}$ is shown in (a). Small circles represent tungsten atoms and large circles represent oxygen atoms. One member from each set of symmetry-equivalent oxygen atoms is labeled, and this labeling scheme is used in (b). The ^{17}O NMR spectrum shown in (b) corresponds to spectrum **19** in Table III.

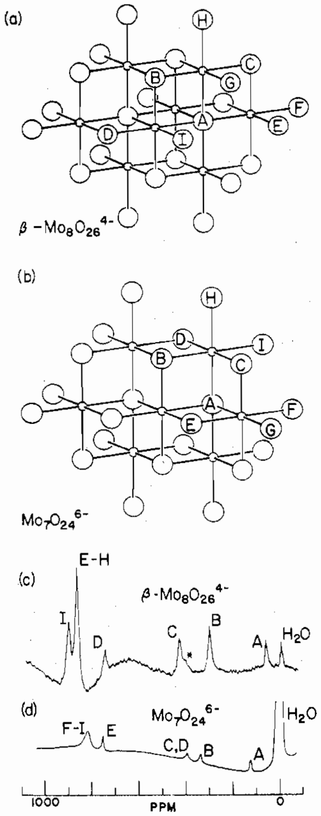

Figure 8. Idealized bond structures of β-$Mo_8O_{26}^{4-}$ (a) and $Mo_7O_{24}^{6-}$ (b). Small circles represent molybdenum atoms and large circles represent oxygen atoms. Within each structure, one member from each set of symmetry-equivalent oxygen atoms is labeled, and these labeling schemes are used in (c) and (d). The ^{17}O NMR spectra shown in (c) and (d) correspond to spectra **20** and **21**, respectively, in Table III. The asterisk in (c) labels the resonance due to α-$Mo_8O_{26}^{4-}$ (see ref 13).

be taken into account if resonances with similar chemical shift values are to be assigned unambiguously. Similar ambiguities exist in the spectrum of $W_{10}O_{32}^{4-}$ (see Figure 7). Here only one OW resonance and two OW_2 resonances are observed although the structure contains two types of OW oxygens and three types of OW_2 oxygens. Comparison of W–O bond

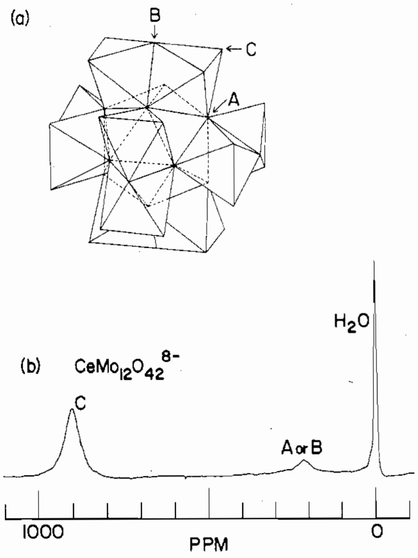

Figure 9. Polyhedral model of the tetrahedral $CeMo_{12}O_{42}^{8-}$ structure is shown in (a). Octahedra outline the octahedral molybdenum coordination polyhedra, two of which are not visible. Only the forward portion of the icosahedral cerium coordination polyhedron is shown, and portions obscured by octahedra are indicated with dashed lines. One member of each set of symmetry-equivalent oxygen atoms is labeled, and this labeling scheme is used in (b). The ^{17}O NMR spectrum shown in (b) corresponds to spectrum **23** in Table III.

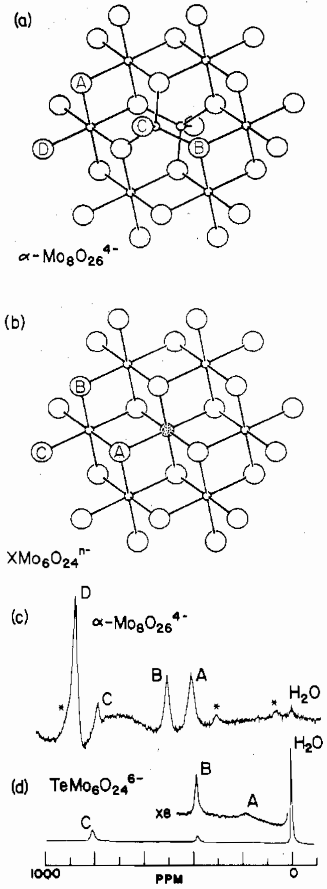

Figure 10. Idealized bond structures of α-$Mo_8O_{26}^{4-}$ (a) and $XMo_6O_{24}^{n-}$ (b). Small open circles represent molybdenum atoms, large open circles represent oxygen atoms, and the shaded circle in (b) represents the X atom. In each structure, one member from each set of symmetry-equivalent oxygen atoms is labeled, and this labeling scheme is used in (c) and (d). In the $H_6XMo_6O_{24}^{n-}$ structure, the O_A atoms in (b) are protonated. The ^{17}O NMR spectra shown in (c) and (d) correspond to spectra **24** and **25**, respectively, in Table III. The asterisks in (c) label resonances due to β-$Mo_8O_{26}^{4-}$ (see ref 13).

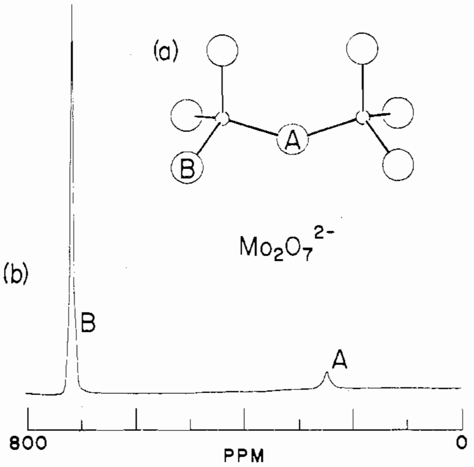

Figure 11. Idealized bond structure for $Mo_2O_7^{2-}$ is shown in (a). Small circles represent molybdenum atoms and large circles represent oxygen atoms. The labels "A" and "B" given in (a) and used in (b) refer to bridging and terminal oxygens, respectively. The spectrum shown in (b) corresponds to spectrum **29** in Table III.

lengths for the OW oxygens in $W_{10}O_{32}^{4-}$ reveals no significant variations, and it is even possible that one of the OW_2 oxygen resonances is not observed.

The reactivity of water toward certain polyoxoanions is illustrated by the aqueous polymolybdate system. When aqueous $Mo_7O_{24}^{6-}$ is acidified stoichiometrically to $Mo_8O_{26}^{4-}$, the ^{17}O NMR spectrum of the resulting solution displays no polyoxoanion resonances. Only a broadened water resonance is observed, indicating rapid oxygen exchange between solvent and solute. This rapid exchange process may be eliminated by measuring the spectrum of the β-$Mo_8O_{26}^{4-}$ ion as a mixed $K^+/(n\text{-}C_4H_9)_4N^+$ salt in CH_3CN (see Figure 8c). Resonances in this spectrum are assigned as follows. The β-$Mo_8O_{26}^{4-}$ ion (see Figure 8a) contains nine types of symmetry-equivalent oxygens: 4 types of cis dioxo OMo oxygens (O_E–O_H), i.e., terminal oxygens bonded to molybdenums having two terminal oxygens; 1 type of monooxo OMo oxygens (O_I), i.e., terminal oxygens bonded to molybdenums having only one terminal oxygen; 2 types of OMo_2 oxygens (O_C, O_D); 1 type of OMo_3 oxygens (O_B); 1 type of OMo_5 oxygens (O_A). The 56 ppm resonance is assigned to the OMo_5 oxygens since all O_A–Mo distances are greater than 2.1 Å. In the terminal oxygen region, the larger 866 ppm resonance is assigned to the 12 cis dioxo terminal oxygens and the smaller 900 ppm resonance is assigned to the two monoxo terminal oxygens. Comparison of the O–Mo bond lengths for the two types of OMo_2 oxygens shows that the O_D oxygens have one very short bond (d_{Mo-O} = 1.75, 2.32 Å) whereas the O_C oxygens have "normal" bond lengths for doubly bridging oxygens (d_{Mo-O} = 1.85–1.95 Å).[61a] The 743 ppm resonance is therefore assigned to the O_D oxygens. Since its value compares well with chemical shift values for other OMo_2 oxygens bonded to *cis*-dioxomolybdenums (see below), the 425 ppm resonance is assigned to the O_C oxygens. The remaining resonance at 296 ppm is then assigned to the OMo_3 oxygens, O_B.

Resonances for the aqueous $Mo_7O_{24}^{6-}$ anion at 25 °C are assigned in an analogous fashion,[71] but the assignments fail to account for the approximately equal intensities of the 398 and 340 ppm resonances (see Figure 8d). This inconsistency may reflect incorrect assignments of these two resonances or may reflect the presence of additional species in solution. When aqueous $Mo_7O_{24}^{6-}$ solutions are heated, all ^{17}O resonances broaden, including the solvent resonance. At about 40 °C, a broad resonance appears at 559 ppm, and when the solution temperature is increased to 50 °C, this new resonance narrows slightly while the remaining resonances broaden. At 90 °C only a very broad water resonance is observed. The entire sequence of temperature-dependent spectral changes is reversible. We have no explanation for these observations which serve only to illustrate the unexpected equilibria and rapid exchange reactions which may complicate the interpretation of aqueous molybdate spectra.

The kinetic inertness of the polyacid $H_8CeMo_{12}O_{42}$ with respect to water oxygen exchange contrasts sharply with the molybdate systems just mentioned. This species requires about 24 h to completely exchange its oxygens with solvent water at 25 °C, and the exchange is accompanied by partial sample decomposition.[72] This inertness may be used to advantage, however, by dissolving enriched compound into unenriched water to obtain aqueous spectra with a solvent resonance having reduced intensity (see Figure 9b). Unfortunately, only two resonances are observed although the compound contains three types of oxygens. This is not surprising in light of the extremely large line widths of the observed resonances.[73]

Rapid exchange processes may occur even in nonaqueous solution. In the case of the α-$Mo_8O_{26}^{4-}$ anion, fully resolved spectra are observed only at low temperatures where the exchange rate is reduced.[15] Both octahedrally and tetrahedrally coordinated molybdenums are present in this anion (see Figure 10a). The terminal oxygen resonances are assigned on the basis of relative intensities, and the bridging oxygen resonances are assigned using bond length data: the bond from each O_B oxygen to the tetrahedrally coordinated molybdenum is much shorter (1.7 Å) than the Mo–O bonds for the O_A oxygens (1.9 Å).[13] Note that these assignments yielded a chemical shift value for O_A oxygens which is very similar to the values observed for O_B oxygens in the structurally related $XMo_6O_{24}^{n-}$ and $H_6XMo_6O_{24}^{n-}$ anions (see Figure 10b,d and Table III)

We mention finally the spectrum of the $Mo_2O_7^{2-}$ anion shown in Figure 11. Of prime interest here is the broadness of the OMo_2 resonance. Since the $Mo_2O_7^{2-}$ is a small anion and the OMo resonance is quite narrow, the large line width is probably the result of a large electric field at the bridging oxygen site.

Conclusions

In this paper we have attempted to demonstrate the feasibility and practicality of observing and assigning ^{17}O resonances from a wide variety of structurally characterized, diamagnetic polyoxoanions. Future publications will compare the data obtained in order to establish chemical shift scales and deal in detail with applications of the ^{17}O NMR technique to problems which have been briefly communicated elsewhere. These applications include the mechanistic interpretation of dynamic NMR spectra,[13] the detection and interpretation of site-selective oxygen exchange processes which occur slowly on the NMR time scale,[14] the determination of protonation sites in basic polyoxoanions,[14,16] and structure determinations of mixed-metal polyoxoanions.[16] The ^{17}O NMR technique should acquire a far greater range of application as a routine analytical tool in the near future due to the recent commercial availability of high-field NMR spectrometers. High-field spectrometers should dramatically expand the domain of species amenable to investigations by ^{17}O NMR by eliminating the need for high levels of ^{17}O enrichment and providing far greater resolution of severely quadrupole broadened resonances.

Acknowledgment. We are grateful to Mr. I. Miura for measuring ^{17}O NMR spectra and the National Science Foundation for providing financial support.

Registry No. **1** + **2**, 12390-22-6; **3**, 57241-87-9; **4**, 12025-96-6; **5**, 12142-54-0; **6**, 68184-33-8; **7**, 11087-54-0; **8**, 59138-97-5; **9**, 51542-99-5; **10**, 68081-64-1; **11**, 53749-36-3; **12**, 53749-37-4; **13** +

14, 68184-32-7; **15**, 64858-58-8; **16**, 64006-46-8; **17**, 68109-04-6; **18**, 68081-63-0; **19**, 68109-03-5; **20**, 61245-58-7; **21**, 12027-67-7; **22**, 12058-33-2; **23**, 12050-53-2; **24**, 59054-50-1; **25**, 59141-55-8; **26**, 59141-49-0; **27**, 59141-56-9; **28**, 59141-57-0; **29**, 64444-05-9; Nb_2O_5, 1313-96-8; Ta_2O_5, 1314-61-0; V_2O_5, 1314-62-1; Na_2SiO_3, 6834-92-0; Na_2MoO_4, 7631-95-0; Na_2WO_4, 13472-45-2; PCl_5, 10026-13-8; H_3PO_4, 7664-38-2; H_3AsO_4, 7778-39-4; MoO_3, 1313-27-5; $C_6H_5AsO_3H_2$, 98-05-5; $(CH_3)_2AsO_2H$, 75-60-5; $(C_6H_5)_2AsO_2H$, 4656-80-8; $(NH_4)_8CeMo_{12}O_{42}$, 12185-83-0; $Te(OH)_6$, 7803-68-1; $NaIO_4$, 7790-28-5.

References and Notes

(1) Fellow of the Alfred P. Sloan Foundation, 1976–1978.
(2) D. L. Kepert in "Comprehensive Inorganic Chemistry", Vol. 4, J. C. Bailar, H. J. Emeleus, R. Nyholm, and A. F. Trotman-Dickinson, Ed., Pergamon Press, Oxford, 1973, pp 607–672.
(3) (a) J. A. Jackson and H. Taube, *J. Phys. Chem.*, **69**, 1844 (1965); (b) B. N. Figgis, R. G. Kidd, and R. S. Nyholm, *Can. J. Chem.*, **43**, 145 (1965).
(4) A. D. English, J. P. Jesson, W. G. Klemperer, T. Mamouneas, L. Messerle, W. Shum, and A. Tramontano, *J. Am. Chem. Soc.*, **97**, 4785 (1975).
(5) M. Filowitz, W. G. Klemperer, L. Messerle, and W. Shum, *J. Am. Chem. Soc.*, **98**, 2345 (1976).
(6) M. Filowitz and W. G. Klemperer, *J. Chem. Soc., Chem. Commun.*, 233 (1976).
(7) O. Lutz, W. Nepple, and A. Nolle, *Z. Naturforsch., A*, **31**, 1046 (1976).
(8) M. A. Fedotov, A. M. Golubev, and L. P. Kazanskii, *Izv. Akad. Nauk SSSR, Ser. Khim.*, 2840 (1976).
(9) M. Filowitz and W. G. Klemperer, *J. Chem. Soc., Chem. Commun.*, 201 (1977).
(10) L. P. Kazanskii, M. A. Fedotov, and V. I. Spitsyn, *Dokl. Akad. Nauk SSSR*, **233**, 152 (1977).
(11) L. P. Kazanskii, *Koordinat. Khim.*, **3**, 327 (1977).
(12) L. P. Kazanskii, M. A. Fedotov, and V. I. Spitsyn, *Dokl. Akad. Nauk SSSR*, **234**, 1376 (1977).
(13) V. W. Day, M. F. Fredrich, W. G. Klemperer, and W. Shum, *J. Am. Chem. Soc.*, **99**, 952 (1977).
(14) W. G. Klemperer and W. Shum, *J. Am. Chem. Soc.*, **99**, 3544 (1977).
(15) V. W. Day, M. F. Fredrich, W. G. Klemperer, and W. Shum, *J. Am. Chem. Soc.*, **99**, 6146 (1977).
(16) W. G. Klemperer and W. Shum, *J. Am. Chem. Soc.*, **100**, 4891 (1978).
(17) P. Model, L. Ponticorvo, and D. Rittenberg, *Biochemistry*, **7**, 1339 (1968).
(18) B. E. Conway, R. E. Verrall, and J. E. Desnoyers, *Trans. Faraday Soc.*, **62**, 2738 (1966).
(19) C. M. Flynn, Jr., and G. D. Stucky, *Inorg. Chem.*, **8**, 178 (1969).
(20) W. H. Nelson and R. S. Tobias, *Inorg. Chem.*, **2**, 985 (1963).
(21) E. O. North and W. Haney, "Inorganic Synthesis", Vol. I, McGraw-Hill, New York, N.Y., 1939, p 127.
(22) Reference 21, p 129.
(23) (a) R. Contant, J. M. Fruchart, G. Hervé, and A. Tézé, *C.R. Hebd. Seances Acad. Sci., Ser. C*, **278**, 199 (1974); (b) A. Tézé and G. Hervé, *J. Inorg. Nucl. Chem.*, **39**, 999 (1977).
(24) H. Wu, *J. Biol., Chem.*, **43**, 189 (1920).
(25) We employ the α–β nomenclature proposed by M. T. Pope, *Inorg. Chem.*, **15**, 2008 (1976).
(26) H. Debray, *C.R. Hebd. Seances Acad. Sci.*, **78**, 1408 (1874).
(27) K. M. Barkigia, L. M. Rajkovič, M. T. Pope, and C. O. Quicksall, *J. Am. Chem., Soc.*, **97**, 4146 (1975).
(28) J. Fuchs, *Z. Naturforsch., B*, **28**, 389 (1973).
(29) B. Grüttner and G. Jander in "Handbook of Preparative Inorganic Chemistry", Vol. 2, G. Brauer, Ed., Academic Press, New York, N.Y., 1965, pp 1710–1711.
(30) P. Baidala, E. A. Torchenkova, and V. I. Spitsyn, *Dokl. Akad. Nauk SSSR*, **196**, 1344 (1971).
(31) Z. F. Shakhova and S. A. Gavrilova, *Zh. Neorg. Khim.*, **3**, 1370 (1958).
(32) L. C. W. Baker, G. A. Gallagher, and T. P. McCutcheon, *J. Am. Chem. Soc.*, **75**, 2493 (1953).
(33) S. R. Wood and A. Carlson, *J. Am. Chem. Soc.*, **61**, 1810 (1939).
(34) Reference 29, p 1738.
(35) G. A. Tsigdinos, Ph.D. Thesis, Boston University, Boston, Mass., 1961.
(36) (a) M. J. Stevenson and C. H. Townes, *Phys. Rev.*, **107**, 635 (1957); (b) R. A. Kamper, K. R. Lea, and C. D. Lustig, *Proc. Phys., Soc., London, Sect. B*, **70**, 897 (1957).
(37) A. O. Nier, *Phys. Rev.*, **77**, 789 (1950).
(38) A. Abragam, "The Principles of Nuclear Magnetism", Oxford University Press, London, 1961, p 314.
(39) Reference 38, p 300.
(40) W. G. Klemperer, *Angew. Chem.*, **90**, 258 (1978); *Angew. Chem., Int. Ed. Engl.*, **17**, 246 (1978).
(41) Although the $Mo_6O_{19}^{2-}$ anion deviates significantly from octahedral symmetry in the solid state,[42] we have seen no manifestation of this distortion in NMR spectra, indicating that the anion is either octahedral or fluxional in solution.
(42) H. R. Allcock, E. C. Bissell, and E. T. Shawl, *Inorg. Chem.*, **12**, 2963 (1973).
(43) J. Fuchs, W. Freiwald, and H. Hartl, *Acta Crystallogr., Sect. B*, **34**, 1764 (1978).
(44) I. Lindqvist, *Ark. Kemi*, **5**, 247 (1953).
(45) I. Lindqvist and B. Aronsson, *Ark. Kemi*, **7**, 49 (1954).
(46) The $VMo_5O_{19}^{3-}$ and $VW_5O_{19}^{3-}$ anions are assumed to be isostructural since they display the same pattern of IR absorptions in the 650–1200-cm^{-1} region.
(47) C. M. Flynn, Jr., and M. T. Pope, *Inorg. Chem.*, **10**, 2524 (1971).
(48) (a) J. L. Hoard, *Z. Kristallogr., Kristallgeom., Kristallphys., Kristallchem.*, **84**, 217 (1933); (b) A. Ferrari, L. Cavalca, M. Nardelli, O. Scagnioli, and E. Tognoni, *Gazz. Chim. Ital.*, **80**, 352 (1950).
(49) A. Kobayashi and Y. Sasaki, *Bull. Chem., Soc. Jpn.*, **48**, 885 (1975).
(50) J. M. Fruchart, G. Herve, J. P. Launary, and R. Massart, *J. Inorg. Nucl. Chem.*, **38**, 1627 (1976).
(51) (a) R. Strandberg, *Acta Chem. Scand., Ser. A*, **29**, 359 (1975); (b) R. Allmann, *Acta Chem. Scand., Ser. A*, **30**, 152 (1976); (c) H. D'Amour and R. Allmann, *Z. Kristallogr., Kristallgeom., Kristallphys.*, **143**, 1 (1976).
(52) G. M. Brown, M. R. Noe-Spirlet, W. R. Busing, and H. A. Levy, *Acta Crystallogr., Ser. B*, **33**, 1038 (1977).
(53) Similar effects have been observed in ref 7 and 16.
(54) L. Barcza and M. T. Pope, *J. Phys. Chem.*, **79**, 92 (1975).
(55) S. W. Rabideau and H. G. Hecht, *J. Chem. Phys.*, **47**, 544 (1967).
(56) H. D'Amour, *Acta Crystallogr., Sect. B*, **32**, 729 (1976).
(57) The structure of β-$P_2W_{18}O_{62}^{6-}$ is uncertain. Compare K. Y. Matsumoto and Y. Sasaki, *J. Chem. Soc., Chem. Commun.*, 691 (1975), and R. Massart, R. Contant, J. M. Fruchart, J. P. Ciabrini, and M. Fournier, *Inorg. Chem.*, **16**, 2916 (1977).
(58) (a) M. T. Pope, C. O. Quicksall, W. Kwak, L. M. Rajkovic, J. K. Stalick, K. M. Barkigia, and T. F. Scully, *J. Less-Common Met.*, **54**, 129 (1977); (b) M. T. Pope, private communication.
(59) T. Nishikawa and Y. Sasaki, *Chem. Lett.*, 1185 (1975).
(60) J. Fuchs, H. Hartl, W. Schiller, and U. Gerlach, *Acta Crystallogr., Sect. B*, **32**, 740 (1976).
(61) (a) H. Vivier, J. Bernard, and H. Djomma, *Rev. Chim. Miner.*, **14**, 584 (1977); (b) B. M. Gatehouse, *J. Less-Common Met.*, **54**, 283 (1977); (c) L. O. Atovmyan and O. N. Krasochka, *Zh. Strukt. Khim.*, **13**, 342 (1972).
(62) (a) K. Sjobom and B. Hedman, *Acta Chem. Scand.*, **27**, 3673 (1973); (b) H. T. Evans, Jr., B. M. Gatehouse, and P. Leverett, *J. Chem. Soc., Dalton Trans.*, 505 (1975).
(63) D. D. Dexter and J. V. Silverton, *J. Am. Chem. Soc.*, **90**, 3589 (1968).
(64) J. Fuchs and H. Hartl, *Angew. Chem.*, **88**, 385 (1976); *Angew. Chem., Int. Ed. Engl.*, **15**, 375 (1976).
(65) H. T. Evans, Jr., *Acta Crystallogr., Sect. B*, **30**, 2095 (1974).
(66) Assumed to be isostructural with $H_6CMo_6O_{24}^{3-}$ (see ref 65): A. Perloff, *Inorg. Chem.*, **9**, 2228 (1970).
(67) (a) H. J. Becher, H. J. Brockmeyer, and U. Prigge, *J. Chem. Res. (S)*, 117 (1978); *J. Chem. Res. (M)*, 1670 (1978); (b) K. Stadnicka, J. Haber, and R. Kozlowski, *Acta Crystallogr., Sect. B*, **33**, 3859 (1977); (c) ref 61b.
(68) We do not believe that this broadening is caused by large electric field gradients at the oxygen sites because the coordination geometries of the W and O atoms in α-$P_2W_{18}O_{62}^{4-}$ are very similar to those in $W_6O_{19}^{2-}$, $SiW_{12}O_{40}^{4-}$, and $PW_{12}O_{40}^{3-}$. These smaller species display much narrower resonances (see above).
(69) Differences in electric field gradient values may also play a role here.
(70) M. T. Pope, private communication. These differences in average bond lengths are not statistically significant.
(71) See ref 40 for a detailed discussion.
(72) Sample decomposition was detected by the appearance of new bands in aqueous IR spectra.
(73) The possibility of selective enrichment cannot be ruled out, but the use of enriched solvent does not lead to the appearances of any new resonances.
(74) Coordinates from ref 52 for α-$PW_{12}O_{40}^{3-}$.